

FEDSM-ICNMM2010-30) &

AERODYNAMIC PARTICLE RESUSPENSION DUE TO HUMAN AND MODEL FOOT MOTIONS

Yoshihiro Kubota

Graduate School of Engineering
Toyo University
2100 Kujirai, Kawagoe, Saitama 350-8585, Japan

Hiroshi Higuchi

Department of Mechanical and Aerospace
Engineering
Syracuse University
Syracuse NY 13244, USA

ABSTRACT

Human foot motions such as walking and foot tapping detach the particulate matter on the floor and redistribute it, increasing the particle concentration in air. The objective of this paper is to experimentally investigate the mechanism of particle resuspension and redistribution due to human foot motion.

In particular, generation and deformation of vortex produced by the foot motion and how they are affected by the shape of sole have been examined. The experiments were carried out by particle flow visualization and the Particle Image Velocimetry (PIV) measurements in air, and dye flow visualization in water. The flow visualizations with human foot tapping and stomping were also carried out in order to elucidate the particle resuspension in real situations. In a laboratory experiment, the foot was modeled either as an elongated plate or a foot wearing a slipper, moving normal to the ground downward or upward. To focus on the aerodynamic effect, the model foot was stopped immediately above the floor before contacting the floor. The results indicated that the particles were resuspended both in downward motion and in upward motion of the foot. The particle resuspension and redistribution were associated with the wall jet between the foot and floor and the vortex dynamics. With an elongated plate, three-dimensional vortex structure strongly affected the particle redistribution.

NOMENCLATURE

D	Effective diameter
W	Width of the idealized foot
L	Length of the idealized foot
Z	Gap in motion
Z_i	Initial gap in motion
Z_f	Final gap in motion
Acc	Acceleration in motion

Dec	Deceleration in motion
U	Foot velocity
U_c	Constant foot velocity
t	Time, sec
t_{dur}	Total duration of foot motion
T	Normalized time, $U_c t/D$
T_1	Timing at the end of acceleration phase
T_2	Timing at the end of constant velocity phase
T_3	Timing at the end of deceleration phase
T_{final}	5 sec. after T_3
ν	Kinematic viscosity
Re_{U_c}	Reynolds number based on disk diameter, $U_c D/\nu$

1. INTRODUCTION

An amount of particulate matter (PM) suspended in the air affects the air quality[1]. Walking and other human activities in the room are known to cause elevated concentration of dust suspended in indoor air. The particulate matter is first detached and resuspended from the floor, and then entrained into the human thermal plume, where it can ultimately be inhaled. Ferro et al. 2004, Long et al. 2000 obtained the particle size and mass of resuspended particle with the human activities [2, 3]. Aerosol concentrations and particle size distributions were measured both indoors and outdoors were by Thatcher et al. (1995) [4] and they studied the resuspension of particle, mass loading of dust on floor surfaces and deposition velocity of particle. Abt et al. (2000) examined the contribution of outdoor and indoor particle sources to indoor concentration parameters affecting indoor exposures [5]. In spite of global effect of the walking on the particle concentration, detailed mechanism of how the human motion causes the resuspension of particles has not been elucidated.

Predicting the particle resuspension poses challenges because the particles are strongly attracted to the floor via

various forces (adhesion, electrostatic, Van Der Waals[6] and can be detached via either ballistic or aerodynamic mechanism[7], or combination of both. The ballistic mechanism occurs when colliding particles break the cohesive bond which exists between particles. The aerodynamic mechanism takes place when the particles are resuspended purely by flow disturbances generated by the body such as foot motion. The vortex dynamics around a sphere impacting the wall was studied by Leweke et al. (2004)[8] and the associated dust resuspension investigated by Eames et al. (2000)[7]. The particles resuspension due to a vertically travelling disk was studied experimentally by Kubota et al [9]. Khalifa et al. (2007)[10] studied analytically and numerically the aerodynamic resuspension mechanism of particle attached to the wall beneath a falling disk. DeGraw et al. [11] carried out the numerical investigation paralleling the disk experiment [9] and the present experiment with an elongated plate.

The present paper examines the particle suspension due to actual foot motion (foot tapping and stomping) as well as model foot undergoing a simulated vertical foot motion. As a follow up on our previous study using a disk geometry [9] we examine the three-dimensional geometric effect as well as human foot motion. As was the case in the previous study, the laboratory test focuses on aerodynamic mechanism of particle resuspension avoiding floor vibration, etc. The wall jet and the vortex dynamics caused by the idealized foot motion are measured with the particle image velocimetry. Also, this article addresses the subsequent redistribution of the particles by the aerodynamic mechanism.

In the present laboratory experiment an idealized foot motion is used since modeling the human walking motion and its associated foot kinetics is extremely complex [12] with both a vertical and a rotational component. As a first approximation, the stepping motion is modeled as normal motion to the floor, and both the downward and upward portion of the foot stomping are examined. In these experiments, the motion is stopped just before touching the floor to focus on the aerodynamic resuspension mechanism, ensuring no floor vibration. Here, the idealized foot is modeled as an elongated plate with the equivalent area to a US 8 size human shoe and a foot model wearing an indoor slipper.

The following sections present the observation of particle resuspension due to human foot motion (Section 2), and velocity measurements and particle visualizations from an elongated plate and from a foot model wearing a slipper (Section 3). The results are discussed in Section 4.

2. PARTICLE VISUALIZATION OF HUMAN FOOT MOVEMENT

2.1 Experimental Procedure

Particle flow visualizations with an actual foot tapping and stomping were first conducted. These two modes focus on the rotation and vertical motion of the foot, and may be regarded as major elements in the walking process. The subject wore an

indoor slipper with a smooth sole during both tapping motion and stomping motion. The foot position and velocity were recorded with a Photron high-speed camera and analyzed on the computer. A foot tapping motion consisted of foot pivoting around the heel touching the floor. The foot stomping motion consisted of the vertical motion; the sole was set parallel to the wall during the motion. Particle resuspension from the smooth hard surface due to the human foot motion was recorded as follows: 3M Ceramic Microspheres G-200 with a mean diameter of $8\mu\text{m}$ were uniformly distributed underneath the foot prior to the foot motion. The typical initial density of seeding was $5.6\text{mg}/\text{cm}^2$. The Photron camera was operated at 125 frames per second to take the images. The flow-field was illuminated in its cross section with a thin laser sheet from an Argon ion laser beam.

2.2 Results of Particle Resuspension by Human Foot Tapping and Stomping

The effect of the foot tapping was studied first. Vertical positions of the toe and mid sole were recorded and are shown in Fig. 1. The angular velocity was approximately 5 rad/s when the foot contacted the floor. The sequence of particle flow visualization with an actual foot tapping motion is shown in Fig. 2. The toe is facing the reader in the sequence of figures. The time increment is 0.1 sec. The foot stopped from downstroke motion at $t=0\text{sec}$. (Fig. 2a), and following two images show the results during the upstroke motion. The particles that were

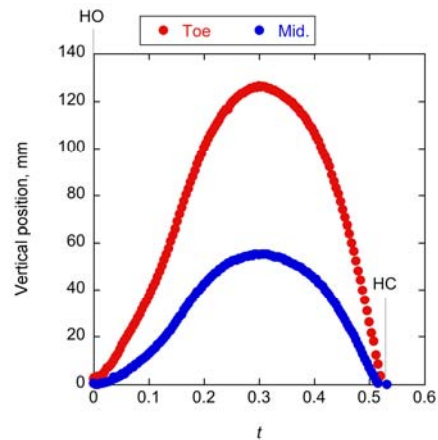


FIGURE 1: TIME HISTORY OF VERTICAL POSITION OF TOE AND MID SOLE DURING FOOT TAPPING.

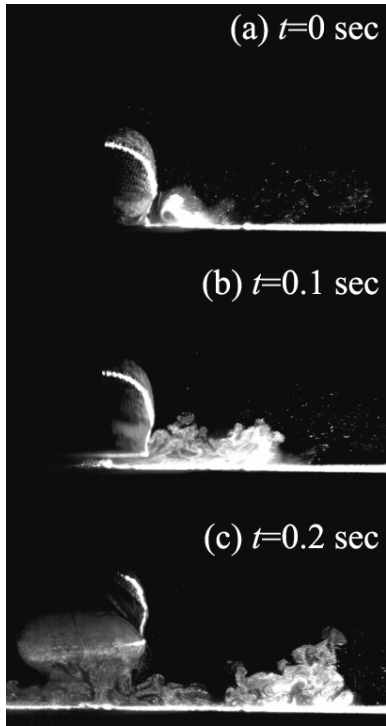


FIGURE 2: PARTICLE FLOW VISUALIZATION OF FOOT TAPPING ILLUMINATED ON MID-SECTION. THE TOE IS FACING THE READER AND IN AN UPWARD MOTION.

initially seeded beneath the foot were expelled from the floor and entrained into the vortex at $t=0$ sec. Later at $t=0.1$ sec. (Fig. 2b), the resuspended particles were driven out further out to the side. The result at $t=0.2$ sec clearly shows the particle resuspension and redistribution processes. In upward motion, the particles were also resuspended in the wake behind under the foot at $t=0.2$ sec (Fig. 2c). Thus, these figures show that both downstep and upstep motions are equally important for the resuspension and redistribution of particles.

The foot stomping motion was examined with the high-speed camera next. Time history of the foot position and that of the velocity near the wall are shown in Fig. 3a and 3b, respectively. Note the foot decelerates slightly before it impacts the floor. The overall movement of the foot and its velocity time history were later incorporated into the laboratory experiment as shown in Fig. 7. The results of particle flow visualization with the stomping motion are shown in Fig. 4 and Fig. 5. These results were taken 0.2 sec after the foot stopped in downstroke motion. As before, the particles were initially seeded beneath the foot. The subject wore an indoor slipper. In Fig. 4, the toe is facing the reader and the laser light sheet illuminate the mid section of the lateral particle flow motion. Fig. 5 shows the resuspension of particles from the toe in the longitudinal cross section. The particles were expelled from the floor in both directions of foot as evidenced in these figures. Three-dimensional particle resuspension patterns were examined more in detail with the model foot as described later.

The resuspended particles became entrained into the vortex structure around the foot. The size of vortex core also varied around the foot, e.g., the mid-section of the foot (Fig. 4) produced a larger vortex than the front of the toe (Fig. 5). Thus, the resuspension and redistribution of particles would be affected with the geometry of sole. To understand the process of particles resuspension and redistribution from the three-dimensional geometry beyond our previous study using an axisymmetric geometry [9] in more detail, the experiments were carried out using an idealized foot in prescribed motion, and are described in the next section.

3. LABORATORY EXPERIMENT ON SIMULATED FOOT MOTION

3.1 Set up

The particle resuspension study with the actual foot motion was followed up in the laboratory setting to maximize the measurement accuracy and repeatability and to examine the detailed mechanism of the particle resuspension process. The axisymmetric velocity vector field and particle resuspension phenomena caused by a disk in both downward and upward

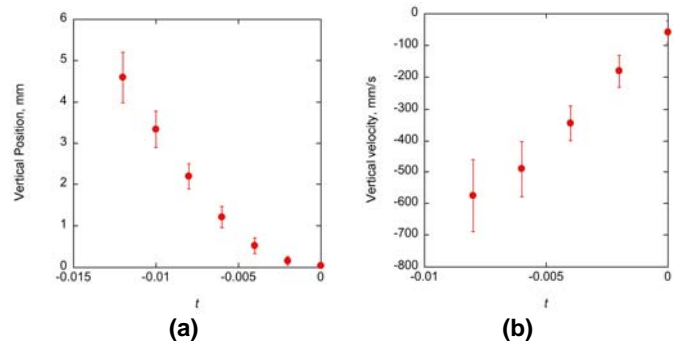


Figure 3: (a) TIME HISTORY OF FOOT POSITION NEAR THE WALL DURING THE FOOT STOMPING (b) VERTICAL VELOCITY TIME HISTORY NEAR THE WALL DURING THE DOWNSTROKE OF THE STOMPING (In this figure the negative velocity indicates motion toward the wall.)



FIGURE 4: PARTICLES FLOW VISUALIZATION WITH A MID-SECTION OF FOOT STOMPING.



FIGURE 5: PARTICLES FLOW VISUALIZATION WITH AN ACTUAL FOOT STOMPING OF TOE.

motion have been examined and reported earlier [9]. Focus of the present study was on the three dimensional effects due to geometry that was more representative of shoes than a canonical disk geometry. Here, two different geometries were used: (1) an elongated plate and (2) an indoor slipper. All had smooth bottom surface. The geometry of the elongated plate was a rectangle with two half circles at both ends: the overall dimensions are 71.7mm in width (W) and 269.8mm in length (L). The idealized foot motions were driven vertically by a computer-controlled linear servo motor. The setup for an idealized foot experiment was the same as that used in the disk experiment [9] and is shown schematically in Fig. 6. The motion was controlled by specifying the maximum velocity, acceleration, deceleration and stroke. Both the flow visualization and the flow-field velocity measurement were conducted in a 1.2m x 1.2m sealed acrylic case to ensure that no cross-flow drafts were present.

An actual foot stomping motion was recorded as mentioned above, and a sample velocity time history of the idealized foot motion used is shown in Fig. 7, that consists of three phases: acceleration from rest, constant velocity and deceleration to rest and approximate the actual human foot stomping motion. The details of the motion are shown parametrically in Table 1. An initial gap in motion (Z_i), a final gap in motion (Z_f) and a Reynolds number (Re_{U_c}) were specified and two different sets of parameters were selected for the investigation. In order to focus on the aerodynamic effects, the model was stopped 0.1mm above the acrylic floor without causing any floor vibration.

Particle flow visualization was conducted with the same condition as in the foot tapping and stomping such as a seeding, a laser sheet and a high speeds camera. In addition, a high definition SONY Camcorder (HDR-HC3) operating at 30 frames per second was used to take the images during the upward motion to get wider viewing area and higher image sensitivity.

A Dantec two-component Particle Image Velocimetry (PIV) system was used for quantitative velocity measurements. Seeding was provided by a Laskin-nozzle type seeder (TSI Model 9307) with olive oil (nominal droplet size 1-5 μm in

diameter). The flow field was illuminated in its cross-section with a thin laser light sheet from a Nd:YAG laser beam. The PIV image acquisition was triggered at various locations of the stepping cycle so that the results could be phase-averaged. The results were averaged from 50 images yielding the standard deviation 13.3% in the phase-averaged velocity.

A supplementary experiment was also carried out in water to study the evolution of the three-dimensional vortex ring and described in the results section.

3.2 Results of PARTICLE RESUSPENSION WITH AN ELONGATED PLATE

DOWNSTROKE

The particle streak pattern left by an elongated plate after the downward motion is shown in Fig. 8. The idealized motion simulated the downward stomping motion shown in Fig. 7. The parameters of motion are listed in Table 1. The particles were initially seeded beneath the foot, and the initial seeding pattern was in the same as the elongated pate. As observed under a disk [9], the particles were expelled under the foot by an unsteady

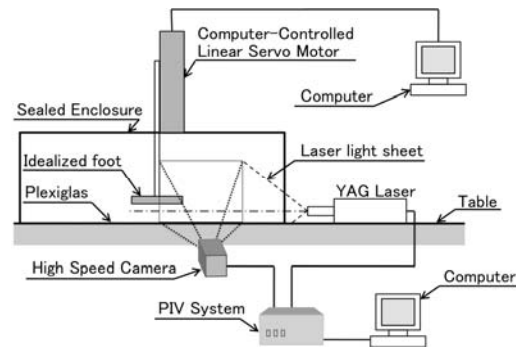


FIGURE 6: IDEALIZED FOOT EXPERIMENT SETUP.

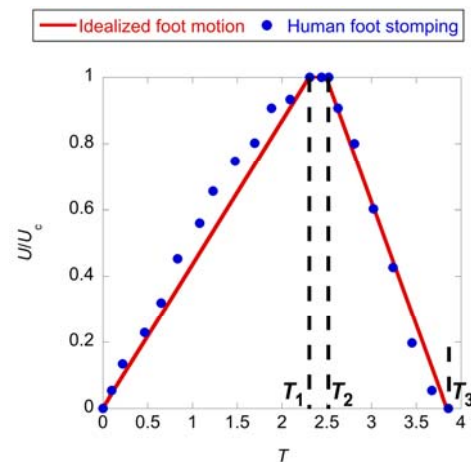


FIGURE 7: VELOCITY TIME HISTORIES OF THE ACTUAL FOOT STOMPING AND THE IDEALIZED MOTIONS.

Case	Downstroke Stomping	Upstroke Stomping
U_c [m/s]	1.875	1.725
Z_i [mm]	300	0.1
Z_f [mm]	0.1	300
Acc [m/s ²]	10.60	13.86
Dec [m/s ²]	-16.02	-9.55
T_1	2.18	1.41
T_2	2.34	1.65
T_3	3.78	3.69
t_{dur} [sec]	0.307	0.326
T_{final}	65	65
Re_{Uc}	18,500	17,500

TABLE 1: PARAMETERS USED FOR STOMPING.

wall jet. On the other hand, the strongly directional particles pattern can be seen at the mid-section of foot. Streaks in the particle patterns are believed to be associated with the flow instability as well as the particle interactions as seen beneath the disk. Additional particle flow visualizations were carried out to study the effect of initial particle position on particle resuspension, i.e., to study where the resuspended particles came from. Figures 9 show the final particle distributions for three different types of initial seeding patterns. These included the particles spread over up to $W/8$ from the edge of the foot beneath the foot in a racetrack pattern (b) and particles seeded beneath the foot up to $W/4$ from the edge of the foot(c). Figure 8 is reproduced as Fig. 9(a) as a reference. The initial positions of particles clearly affected the particle redistribution. Particles near the edge and the mid-section of foot were expelled more significantly and the rest of the particles was left underneath the foot. The particles did not escape from the center of the foot (see Fig.9(c)). This phenomenon was also observed with the disk foot experiment. The particle flow visualizations in side view cross-sections, in both longitudinal direction and lateral directions, are shown in Fig. 10 during the downward stomping motion. The initial seeding pattern was just underneath the foot, and all of experiment conditions were the same as the results of bottom view in Fig. 8. (The geometrical details of the foot model assembly are also visible in the figure: the foot was attached to a flange, 50mm in diameter that was connected to the rod fixed to the linear servo-motor. The thicknesses of foot and flange were both 12.7mm.) The particles were expelled more in the lateral direction from under the foot and resuspended, then redistributed away from the floor. As in the case of the particle resuspension underneath the disk [9], the cause of particle resuspension was associated with the wall jet beneath the foot, and the redistribution is associated with the vortex dynamics. The scale of vortex was larger in the lateral

direction than in the longitudinal direction. Also, these results agreed with the results of an actual foot motion: the vortex dynamics associates the redistribution of particles, the larger scale of vortex was evident in the mid-section of foot. The associated flowfield was investigated quantitatively next with the PIV system.

The velocity field measurements with the elongated plate during downstroke stomping motion are shown in Fig. 11. The foot is masked in black. The smaller scale vortex is seen in the longitudinal direction in Fig. 11(a), and this vortex has been shown with the results of particles flow visualization in Fig. 10(a). Also, the resuspended particles were entrained into the vortex near the edge of foot in Fig. 10(a). In lateral direction, the larger scale vortex is seen in Fig. 11(b). This larger scale vortex is also evident in the particle flow visualization in Fig. 10(b). The high velocity region is shown in the present larger scale vortex. This high velocity region corresponds to the strong trajectories in mid-section of foot in Fig. 8. The velocity profiles beneath the elongated plate on downward stomping motion are shown in Fig. 12 at $T=3.52$, $z/D=0.052$. The strong wall jet was also observed underneath the disk [9]. In the present case, the velocity of the wall jet underneath the foot and consequently the wall shear stress was larger in the lateral direction (B) than in the longitudinal direction (A), corresponding to more particle resuspension in the lateral direction. The larger velocity may be heuristically explained by the difference in pressure gradient between the stagnation region under the plate and the external region across the varying distance. The vortex dynamics behind the elongated plate is addressed later.

UPSTROKE

The results of particle flow visualization and velocity field measurements during upward motion by the elongated plate are shown in Fig. 13. The masked areas in Fig. 13(a-i) and Fig. 13(b-i) correspond to the foot. In particle flow visualization, the particles were initially seeded beneath the plate matching the plan form of the plate. In both in longitudinal and

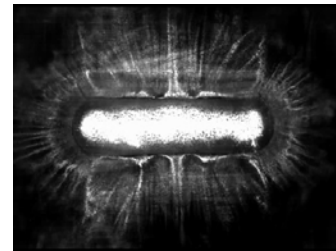


FIGURE 8: PARTICLES TRAJECTORIES WITH AN ELONGATED PLATE FROM BOTTOM VIEW.

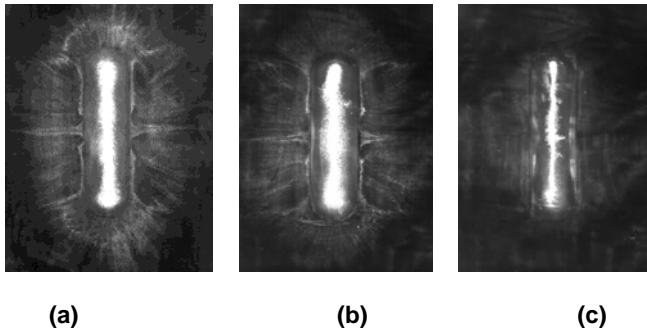


FIGURE 9: PARTICLES TRAJECTORIES WITH DIFFERENT INITIAL SEEDING PATTERN, (A) SAME GEOMETRY AS AN ELONGATED PLATE, (B) SEEDING FROM CENTER OF FOOT TO W/8 FROM THE EDGE OF THE FOOT AND (C) SEEDING FROM CENTER OF FOOT TO W/4 FROM THE EDGE OF THE FOOT.

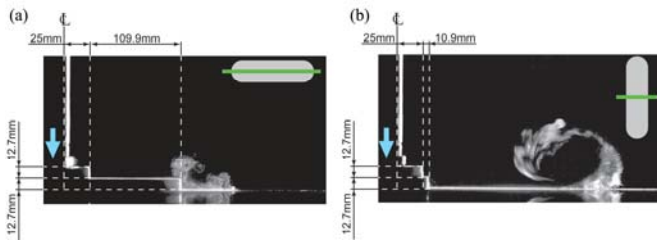


FIGURE 10: PARTICLES FLOW VISUALIZATION IN DOWNSTROKE OF STOMPING MOTION AT $T=4.92$, $Z=Z_f$, (A) LONGITUDINAL DIRECTION AND (B) LATERAL DIRECTION.

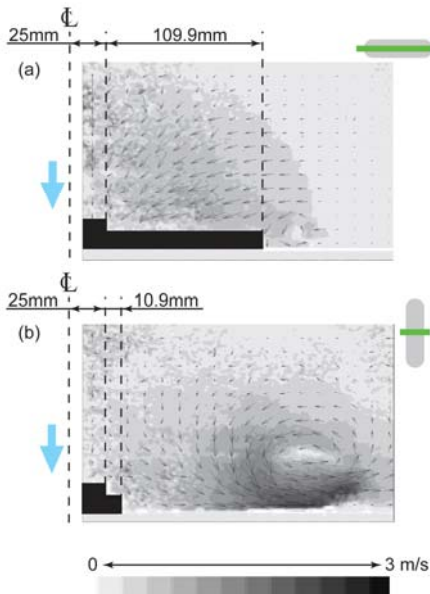


FIGURE 11: VELOCITY MEASUREMENT FOR IN DOWNSTROKE OF STOMPING WITH AN ELONGATED PLATE AT $T=4.92$, $Z=Z_f$, (A) LONGITUDINAL DIRECTION AND (B) LATERAL DIRECTION.

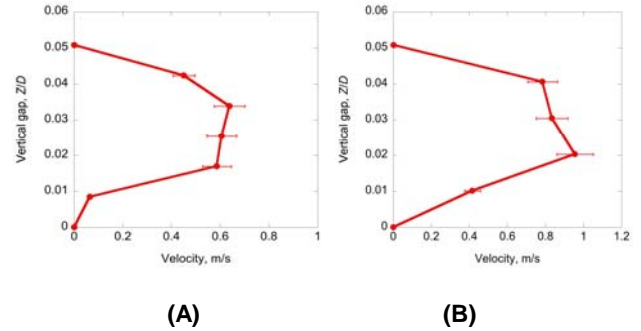


FIGURE 12: VELOCITY PROFILE BENEATH THE ELONGATED PLATE ON DOWNWARD STOMPING MOTION AT $T=3.52$, $Z/D=0.052$: (A) LONGITUDINAL DIRECTION AND (B) LATERAL DIRECTION.

lateral directions, the particles became airborne from the wall. In longitudinal direction in Fig. 13(a-i), the resuspended particles were entrained behind the upward moving foot. In the lateral direction in Fig. 13(b-i), the particles entrained into a more extended region behind the foot. A strong vortex pair can be seen in this cross section. The results of velocity field measurements are shown in Fig. 13(a-ii) and Fig. 13(b-ii). Large concentrations of resuspended particles were located in the high velocity region under the foot in both longitudinal and lateral directions. The present larger scale vortex can be related to the three dimensionality of the vortex deformation. Also, the high velocity region behind the foot would be related to the higher induced velocity by vortex dynamics.

3.3 Supplementary Flow Visualization in Water and Vortex Simulation behind an Elongated Plate

As a supplementary study, vortex formation behind the elongated plate was visualized with dye in the water tank. The fluorescence dye under the UV light was used to illuminate the flow structure. Initially the elongated plate was coated uniformly with the mixed fluorescence and the wake behind the foot during the motion was observed from the top and the side. A Basler A301f camera was operated at 60 frames per second to take the images. The downward foot movement was reproduced with dropping motion.

The results of vortex deformation with the dye flow visualization in water tank simulating the downward stomping motion in side view cross-sections are shown in Fig. 14. The initial height in motion (Z_i), the final gap in motion (Z_f) and Reynolds number (Re_{U_c}) were kept the same with the downward idealized stomping motion in Table 1. The sequence of vortex deformation with the dye flow visualization in the top view is shown in Fig. 14 (a). In the results of the dye flow visualization, at $t=0$ sec., the foot stopped from the downward motion. In $t=-0.5$ sec., the vortex can be seen above the foot which locates in the wake region. In $t=-0.4$ sec., the vortex has started to stretch from the minor axis. At $t=0$ sec., the axis of vortex has switched. This phenomenon of axis switching is agreed with the results of side view (not shown). The vortex

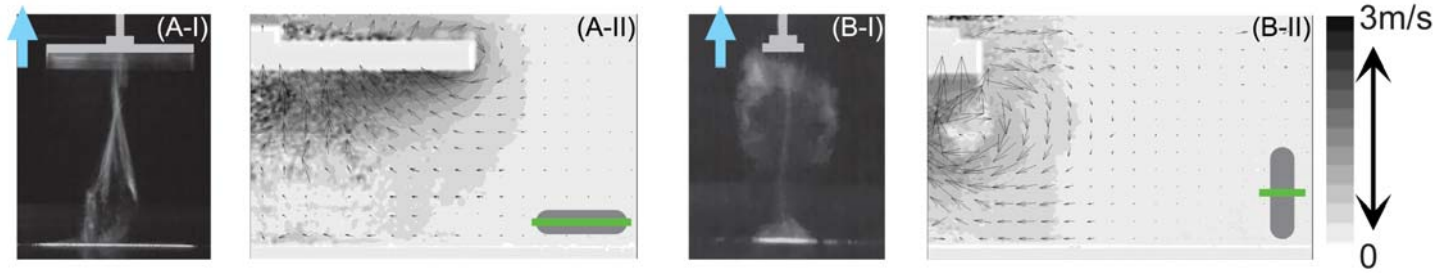


FIGURE 13: PARTICLES FLOW VISUALIZATION AND VELOCITY MEASUREMENTS WITH AN ELONGATED PLATE IN UPSTROKE AT $T=1.6$, $Z/D=0.994$, (A-I) FLOW VISUALIZATION IN LONGITUDINAL DIRECTION, (A-II) MEASUREMENT ON LONGITUDINAL DIRECTION (B-I) FLOW VISUALIZATION ON LATERAL DIRECTION AND (B-II) MEASUREMENT ON LATERAL DIRECTION.

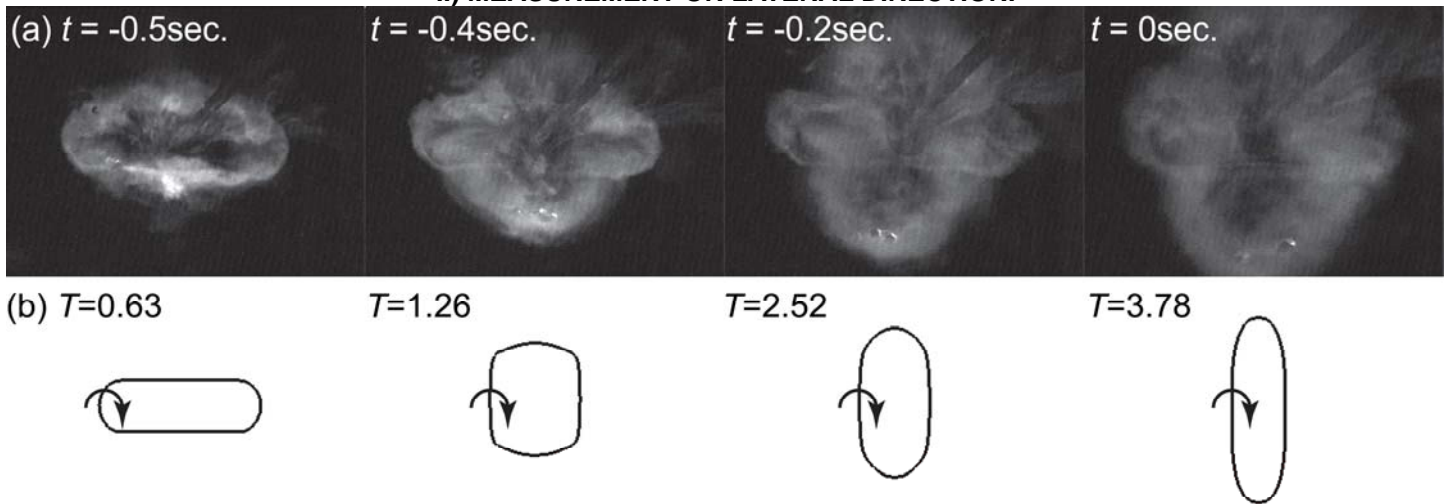


FIGURE 14: (a)SEQUENCE OF DYE FLOW VISUALIZATION ON TOP VIEW WITH AN ELONGATED PLATE IN WATER TANK (b)NUMERICAL SIMULATION OF VORTEX BLOB METHOD.

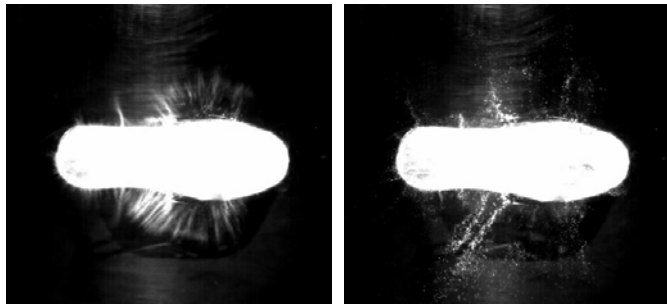


FIGURE 15: PARTICLES TRAJECTORIES WITH A SLIPPER IN DOWNWARD STOMPING MOTION FROM BOTTOM VIEW, (A) $T=3.71$ AND (B) $Z/D=0.001$ AND $T=T_{final}$, $Z=Z_f=0.1\text{mm}$.

continues to stretch in lateral direction after the foot stopped ($t > 0\text{sec}$). The strong streaks from the mid-section of the foot in Fig. 8 are also related to the effect of axis switching of vortex and vortex stretching after the foot stopped. A simple three-dimensional vortex blob method was applied to the present geometry and the sequence of vortex deformation with the

numerical simulation in top view are shown in Fig. 14(b). The computed results clearly showed the out-of plane vortex deformation and the axis switching of vortex, and they were in general agreement with the dye flow visualizations. This supplementary study clarified the deformation of vortex during the foot motion, and also indicated an evolution of vortex geometry to grow in the lateral direction. In short, the elongated plate caused a strong three-dimensional flow which affects the particles redistributions. Wake formations behind a square plate and other polygonal plates were studied by Higuchi et al [13], and the unsteady vortex structure and its interaction with the disk were experimentally and numerically investigated in [14]. Zaman [15] examined the vortex axis switching with an elliptic jet and Hussain et al. [16] studied the deformation of rectangle jets. It is evident that these three-dimensional vortex dynamics play significant role in the present problem.

3.4 Particle Resuspension with a Model Foot Wearing an Indoor Slipper

The particle trajectories underneath commercially available indoor slipper during downward stomping are shown in Fig. 15. The particles were initially seeded just beneath the slipper. In $T=3.71$, the resuspended particles were ejected from the mid-section of the slipper. Later in $T=T_{final}$, particles were redistributed to the diagonal direction in the mid-section of the slipper as shown in Fig. 15(b).

The side cross sectional views of particles resuspended by downward moving slipper are shown in Fig. 16. These results correspond to the typical trajectories in Fig. 15. The result near the heel of slipper is shown in Fig. 16(a), which clearly shows a vortex generating from the heel. In the cross-sectional view at mid-section at a diagonal angle (in Fig. 16(b)) and across the ankle (in Fig. 16(c)), both trajectories show the larger amount of resuspension of particles.

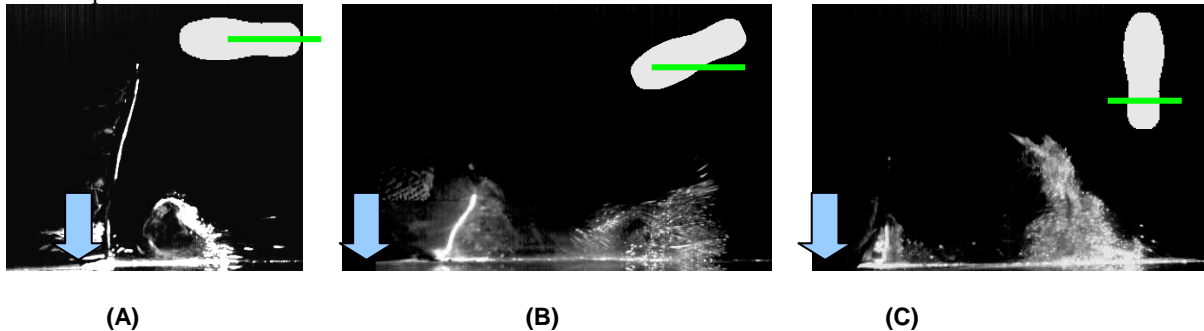


FIGURE 16: PARTICLES FLOW VISUALIZATION FROM SIDE VIEW WITH A SLIPPER IN DOWNWARD STOMPING MOTION AT $Z=Z_f=0.1\text{mm}$, (A) VISUALIZED AT HEEL ON $T=4.27$, (B) VISUALIZED AT MID-SECTION ON $T=4.76$ AND (C) VISUALIZED AT ANKLE ON $T=4.76$.

importance of large-scale flow structures such as the wake vortices for the redistribution of particles over large distance. These cause of the resuspension and redistribution of particles are also observed with the results of disk foot in earlier report [14, 17]. The large-scale flow structures and the particle redistribution are affected by the details of the walking kinematics as well as the sole geometry.

From the results by using an elongated plate and a slipper, the strong three-dimensional aerodynamics effects were clarified during the foot motion. The resuspension and redistribution of particles from mid-section of foot were more significant. In the results with an elongated plate, the strong streaks from mid-section related to the vortex axis switching. The vortex ring dynamics after the foot stopped affects the particle redistribution. Also, the result on upward motion would be related to the vortex axis switching. This three-dimensional vortex dynamics affected the strength of resuspension of particle and redistribution of particle, particularly the latter. With additional forward motion of the foot, the suspended particles will be carried in the wake region behind the foot itself.

In the present experiment, the three-dimensional aerodynamic effect on particle resuspension from a simplified

4. DISCUSSIONS AND CONCLUSIONS

The experiments for the particle resuspension and particle redistribution were carried out with the actual foot tapping, the actual foot stomping and the idealized foot motion. The particle resuspension and particle redistribution occurred during both in upward motion and in downward motion.

In the downward foot motion, the high speed velocity was found in the wall jet between the foot and the floor causing particle resuspension, and the vortex formed in the wake of the foot, resulting in the redistribution of particle. On the upward motion, the particles were resuspended by a wall jet formed by the rapid inflow of air into the low pressure wake region behind the disk. The present results also showed the

elongated plate as well as an actual slipper has been demonstrated. With more realistic shoe geometries, resuspension and redistribution of particles are expected still more three-dimensional and the sole roughness and indentation would play a major role.

ACKNOWLEDGMENTS

This work was carried out at Syracuse University and was supported in part by the New York State STAR Center for Environmental Quality Systems and the U.S. Environmental Protection Agency (US EPA grant/cooperative agreement Award #CR-83199201-0). Although this research has been funded in part by the US EPA, it has not been subjected to the Agency's required peer and policy review; and therefore, does not necessarily reflect the views of the Agency and no official endorsement should be inferred.

REFERENCES

- [1] Nazaroff, W., 2004, "Indoor particle dynamics," *Indoor Air*, 14(s7), pp. 175-183.
- [2] Ferro, A. R., Kopperud, R. J., and Hildmann, L., M., 2004, "Elevated Personal Exposure to Particulate Matter

- From Human Activities in a Residence,” J. Exp. Anal. Environ. Epidemiol, 14, pp. S34-S40.
- [3] Long, C. M., Suh, H. H., and Koutrakis, P., 2000, “Characterization of Indoor Particle Source Using Continuous Mass and Size Monitors,” J. Air Waste Manag. Assoc., 50, pp. 1236-1250.
- [4] Thatcher, T. L., and Layton, D. W., 1995, “Deposition, Resuspension, and Penetration of Particles within a Residence,” Atmos. Environ., 29, pp. 1487-1497.
- [5] Abt, E., Suh, H. H., Catalano, P., and Koutrakis, P., 2000, “Relative Contribution of Outdoor Particles Sources to Indoor Concentrations,” Environ. Sci. Technol., 34, pp. 2579-2587.
- [6] Soltani, M., and Ahmadi, G., 1994, “On Particle Adhesion and Removal Mechanisms in Turbulent Flows,” J. Adhes. Sci. Technol., 8, pp. 763-785.
- [7] Eames, I., and Dalziel, S. B., 2000, “Dust Resuspension by the Flow Around an Impacting Sphere,” J. Fluid Mech., 403, pp. 305-328.
- [8] Leweke, T., Thompson, M. C., and Hourigan, K., 2004, “Vortex Dynamics Associated with the Collision of a Sphere With a Wall,” Physics of fluids, 16, pp. L74-L77.
- [9] Kubota, Y., Hall, J.W. and Higuchi, H., 2009, “An Experimental Investigation of the Flowfield and Dust Resuspension Due To Idealized Human Walking,” J. Fluids Engineering, 131, pp. 081104-1-081104-6.
- [10] Winter, D. A., 2005, “*Biomechanics and motor control of human movement*,” John Wiley & Sons, Hoboken, N.J.
- [11] Khalifa, H. E, and Elhadidi, B., 2007, “Particle Levitation Due to a Uniformly Descending Flat Object,” Aerosol Sci. Technol., 41, pp. 33-42.
- [12] DeGraw, J., Cimbala, J., 2007, “A Lightweight Particle Deposition System for Particle Resuspension Studies,” Presentation at the American Physical Society’s Annual Meeting of the Division of Fluid Dynamics, Salt Lake City, November 18-20.
- [13] Higuchi, H., Anderson, R.W., and Zhang, J., 1996, “Three-Dimensional Wake Formations Behind Regular Polygonal Plates,” *AIAA Journal*, 34(6), pp. 1138-1145.
- [14] Higuchi, H., Balligand, H., and Strickland, J. H., 1996, “Numerical and Experimental Investigations of the Flow Over a Disk Undergoing Unsteady Motion,” J. Fluids Structures, 10, pp. 705-719.
- [15] Zaman, K. B. M. Q., 1996, “Axis switching and spreading of an asymmetric jet: the role of coherent structure dynamics,” J. Fluid Mech., 316, pp. 1-27.
- [16] Hussain, F., Husain, H. S., 1989, “Elliptic jet. Part 1. Characteristics of unexcited and excited jets,” J. Fluid Mech., 208, pp. 257-320.
- [17] Higuchi, H., Transient Flow Fields in Micro and Near Field Human Environment, Seminar 75, IAQ and Ventilation, Conference Proceedings DVD, 2006 ASHRAE Annual Meeting, Quebec City. June 24-28, 2006.